20th International Conference on Renewable Energies and Power Quality (ICREPQ'22)
Vigo (Spain), 27th to 29th July 2022
Renewable Energy and Power Quality Journal (RE&PQJ)
ISSN 2172-038 X, Volume No.20, September 2022

Runner optimal position in a gravitational water vortex hydraulic turbine with a spiral inlet channel and a conical basin

Velásquez García L[1], Rubio-Clemente A[1,2], Chica E[1]

[1] Grupo de Investigación Energía Alternativa, Facultad de Ingeniería, Universidad de Antioquia UdeA, Calle 70, No. 52-21, Medellín, Colombia.

[2]Escuela Ambiental, Facultad de Ingeniería, Universidad de Antioquia UdeA, Calle 70, No. 52-21, Medellín, Colombia.
Phone/Fax number: +57 2195547, e-mail: edwin.chica@udea.edu.co

Abstract. A gravitational water vortex hydraulic turbine (GWVHT) is a low head hydropower technology with a vertical runner for extracting energy from the water vortex. To determine the optimal position (h) of the runner for the hydropower plant efficiency to be increased, a runner in three different positions was compared using computational fluid dynamics (CFD). The position of the runner was a function of the basin height (H). The maximum efficiency (44.15%) was established when the runner was located at 60% of H. The angular velocity associated with the maximum efficiency was 14 rad/s.

Key words. Gravitational water vortex hydraulic turbine, runner, efficiency, hydropower.

1. Introduction

All societies require energy services to serve productive processes and satisfy basic human needs [1]. With a fast increase in economic growth and population, especially in emerging economies, the energy demand is rising rapidly [2]. To provide access to energy services, renewable energy sources will play a key role, being hydroelectric power generation an appealing option [3].

The use of water for the energy generation has been used in the world for many years [4]. Hydropower projects encompass run-of-river and dams with reservoir projects. Hydropower can meet both decentralized rural needs and large centralized urban needs. The power generated in hydroelectric power plants is a function of the water flowing towards the turbine and the head. Hydropower plants can be categorized into large (>10 MW), small (<10 MW), mini (<1 MW), micro (<0.1 MW) and pico (<0.005 MW) hydropower plants [5]. On a large scale, this source of energy has a limited field of expansion, since in developed countries most of the important rivers already have one or several hydropower plants. In turn, in developing countries, large projects can collide with social, financial, and environmental obstacles. As an option, pico, micro, mini and small facilities have been made popular nowadays. These facilities can take advantage of the low flows in rivers without the need to create large dams, limiting the negative environmental effects ascribed to large civil works [6]. New turbines have been added to the conventional turbines for generation in power plants (Pelton, Kaplan and Francis), which can be installed in places where conventional turbines could not operate or operate at very low efficiency, due to their design characteristics. One of those new turbines is the gravitational water vortex hydraulic turbine (GWVHT). This new turbine allows for the generation of electrical energy in rivers with very low falls. Additionally, it can include natural systems, such as rivers or streams or any water network where pipes provide a constant water flow. GWVHTs have an efficiency that varies between 17 and 85% [7]. Despite the advantages, reduced work has been performed on the development and research of GWVHTs. The studies have paid attention generally to the optimization of their geometry to increase the efficiency [7]. For this purpose, it is required to change some geometric parameters of the main turbine components, including the basin, inlet channel or the circulation chamber and the runner.

To contribute to the GWVHT rise efficiency, this work is aiming at determining the optimal position of the runner in the circulation chamber using Computational Fluid Dynamics (CFD). The geometry used was a turbine with a spiral inlet channel and a conical basin.

2. Gravitational water vortex hydraulic turbine

2.1. Inlet channel and basin configuration

GWVHT is an action turbine. In action turbines, the pressure remains constant throughout the runner (atmospheric pressure); therefore, the height of the pressure absorbed by the runner is zero [8]. It is highlighted that the Pelton, Turgo and cross-flow turbines also belong to this group [9]. In a GWVHT, a vortex is induced in the circulation basin when water exits through a hole at its base. The kinetic energy of the vortex is extracted by a vertical axis turbine installed at the vortex centre. The mechanical energy of the runner is converted into electricity by means of the use of a generator. The geometrical configuration used in this study and its dimensions is shown in Fig. 1. The wrap-around inlet or spiral inlet channel is used to design a cyclone separator [10]. For the circulation chamber, cylindrical and conical chambers are normally used [11]. Conical basins are preferred because they produce higher tangential velocity, which represents a higher output-generated power [12]. The geometry of the basin and the inlet channel used was that reported by Velasquez et al. [13].

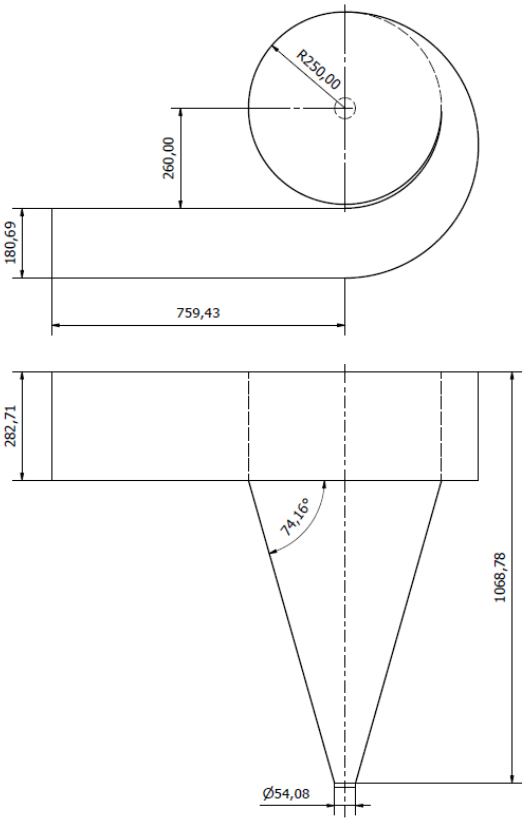

Fig. 1. General view of the GWVHT. Dimensions are expressed in mm.

2.2 Runner configuration

The runner is designed based on an action turbine. The water enters from the channel flow around the basin and drops to a certain height (h). This potential energy is converted into kinetic energy as water swirls around an air core of decreasing radius. If there is more height for the fall of water, then a higher kinetic energy exists. The hydraulic power into the turbine (P) was estimated by Equation 1:

$$P = \rho g h Q \quad (1)$$

where ρ and g refers to the density and gravity, which were set at 998.2 kg/m^3 and 9.81 m^2/s, respectively. In turn, h stands for the water head (m) and Q is the flow rate, which was set at 0.003 m^3/s.

There are different parameters to be considered during the runner design to obtain the maximum power from water. The height and diameters (top and bottom) of the runner, the inlet and the outlet angles, the helical pitch angle, the number of blades and the position in the basin. The height and diameters of the runner, number of blades, inlet, outlet and helical pitch angles were assigned by considering the available literature [14,20, 21,22-24]. During the analysis process, three different positions of the runner were compared. Figure 2 and Table I shows the position used and their hydraulic power. It is noteworthy that the position is a function of the basin height (H). In addition, h is measured to the middle height of the runner.

Table I. Position of the runner and hydraulic power

Run	h	P [w]
1	0.4 H	6.41
2	0.5 H	8.76
3	0.6 H	11.11

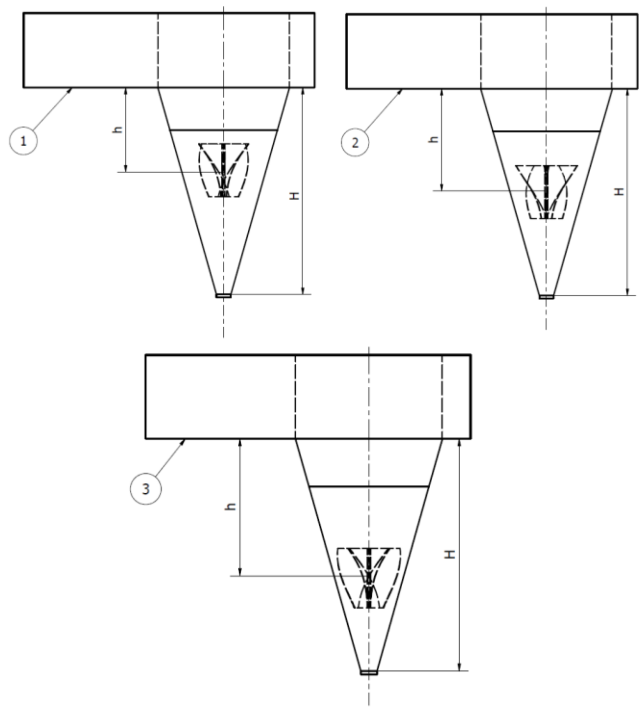

Fig. 2. Different positions of the runner.

Figure 3 shows the velocity triangles for an action turbine. In action turbines, the fluid produces a reaction force on the runner. This force is caused by a change in the momentum on the fluid that is passing through the turbine. The inlet velocity of the fluid (V_θ), in an action turbine, is constant [14]; nevertheless, for the GWVTH, the inlet velocity changes are a function of the vortex radius (*r*), as described by Equation 2:

$$V_\theta = \Gamma / 2\pi r \quad (2)$$

where Γ is the circulation. In Figure 3, v is the absolute velocity, *u* refers to the runner tangential velocity, *R* stands for the fluid relative velocity concerning the runner, v_w is the swirl velocity and subscripts 1 and 2 represent the inlet and outlet, respectively.

Figure 4 illustrates the model of the runner used in this study. In turn, Table II shows the runner characteristics. To determine the diameter of the blades, the diameter of the conical basin at the 3 positions of analysis were considering. It was ensured that with the selected diameters, there was no interference between the rotor and the circulation chamber in any of the analysis positions.

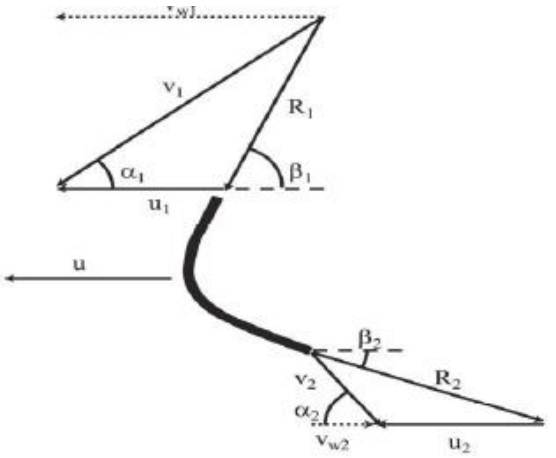

Fig. 3. Velocity triangles for an action turbine [14].

Table II. Characteristics of the runner.

Symbol	Variable	Value
α_1	Blade inlet angle (Deg)	16.00
α_2	Blade outlet angle (Deg)	90.00
β_1	Water inlet angle (Deg)	40.00
β_2	Water outlet angle (Deg)	85.00
λ	Helical pitch angle (Deg)	85.80
L	Blade length (mm)	200
n	Number of blades	4.00
Ds	Top diameter	191.10
Db	Bottom diameter	115.73

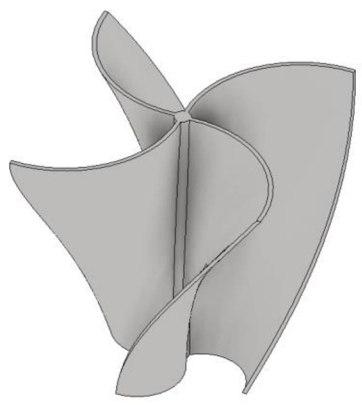

Fig.4. Runner.

3. Numerical analysis

The objective of the simulation is to determine the torque (T) developed by the runner in the given setups at different angular velocities (ω) to calculate the outlet power produced (P_{out}) by the runner and the turbine efficiency (η). The power produced and the efficiency values were calculated by using Equations 3 and 4, respectively:

$$P_{out}=T\omega \quad (3)$$

$$\eta=P_{out}/P \quad (4)$$

The computational analysis was executed using ANSYS Fluent. Two domains were considered: a rotating and a stationary domain in which the runner rotates and the fluid flows, respectively. Figure 5 shows both domains. The meshes were made in Fluent meshing. The poly-hex core mesh was used. Poly-hex core mesh is a novel meshing strategy to solve flow around complex geometries with greater accuracy and speed. This mesh employs polyhedral and hexahedral elements, providing an optimal combination of mesh elements [15]. Additionally, it allows a reduction of approximately 40% in terms of computational time [16].

The Unsteady Reynolds-averaged Navier-Stokes (URANS) equations were solved by employing the coupled scheme for pressure-velocity, and the second-order upwind discretization.

The turbulence was solved using the k-ω SST turbulence model. Furthermore, the volume of fluid (VoF) method was chosen to perform the simulations because multiple fluids were used, including air and water. An inlet velocity (0.059 m/s) was imposed at the inlet channel. For the discharge hole and at the upper surfaces, 0 Pa was used as the relative pressure. For the rotating domain, ω was changed from 0 to 17 rad/s.

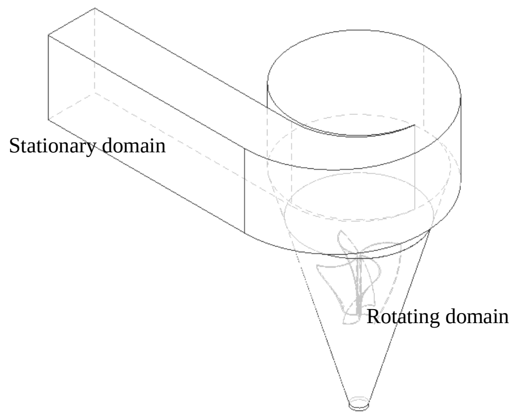

Fig.5. Computational domains.

A mesh independence study was carried out to verify the achievement of the solution convergence. In Table 3, the number of elements used in the mesh independence was shown. The Grid Convergence Index (GCI) method was utilized to define the final mesh [17]. If the value of GCI is close to 1.0, the solution is within the asymptotic range of convergence and the numerical solution does not change with further refinement of the mesh [18]. Additionally, a study of the time-step independence was performed to discern the time-step for the numerical simulations. The time-steps used in the independence study were shown in Table III. The control variable used in these independence tests was T.

After the analysis, the medium mesh and a time-step of 0.0025 s were chosen. The selection of an adequate time-step and mesh reduces the computational time. The computational meshes for the domains are illustrated in Figure 6.

Table III. Grid Convergence Index (GCI).

	Mesh type and GCI	Number of elements	Δt [s]
1	Coarse	524,025	0.005
2	Medium	870,064	0.0025
3	Fine	2,036,661	0.00125
	GCI	0.990	1.002

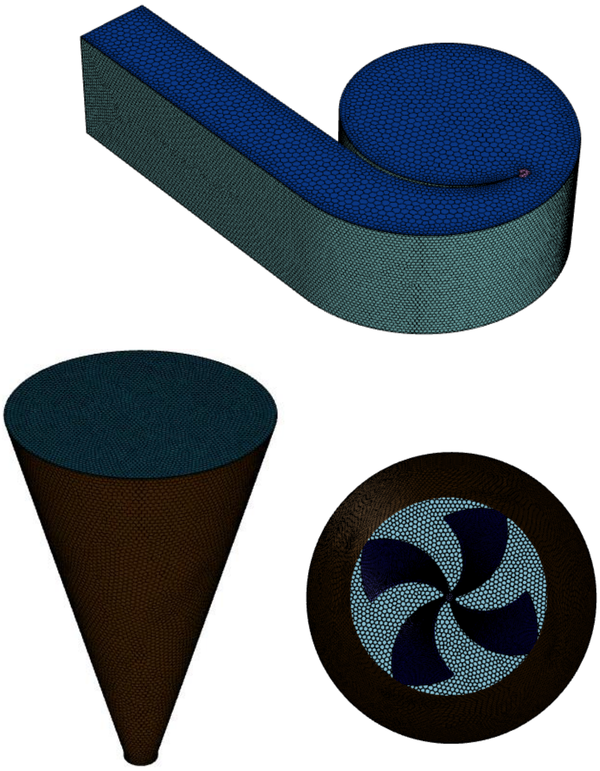

Fig.6. Hex-core mesh.

4. Results and discussion

The results obtained from numerical models are represented in Figure 7 and 8. Figure 7 illustrates the variations in the output mass flow as a function of the time The time needed for the stabilization of the mass flow (constant flow of 3 kg/s) was observed to be close to 30 s for all the analysed models. Figure 8 shows the efficiency of the model as a function of the angular velocity. The efficiency was calculated using the Equation 4. To calculate the outlet power by Equation 3, the values of T and ω were taken of numerical results. The models were not coupled to an electric generator; therefore, the power is only a function of the geometric characteristics of the runner and basin. To quantify the effect of the electric generator on efficiency, it will be necessary, for future work, to specify the type of generator to be used and the way in which this device would be coupled to the turbine, even the material from which the runner was made should be specified.

From Figure 8, Run 3 (h=0.6H) has a maximum efficiency of 44.15%. The runs 1 (h=0.4H) and 2 (h=0.5H) have maximum efficiencies of 6.86 and 30.18%, respectively. The efficiency of the turbine increases as ω is increased and becomes maximal at a ω close to 14 rad/s. Afterwards, the efficiency starts to drop. According to the characteristics of the vortex, the highest ω will be reached near the exit hole [19]; therefore, the closer the rotor will be installed to the exit hole, the higher energy will be available for extraction. Changes of 10% in the location of the runner implied efficiency changes between 13 and 24% for the same runner. Dhakal et al. [11] found a similar conclusion, they concluded that maximum power extraction is possible when the runner position is 65–75% of total heigh to the basin from top position. However, the authors use a runner with curved blades aligned with the turbine axis, that is, without helical pitch angle, and do not specify the geometric characteristics of the runner, so a direct comparison with the present study is not possible. Whether more factors are included in the study of the rotor efficiencies, such as the inlet and the outlet angles, and the number of blades, the efficiencies could increase considerably.

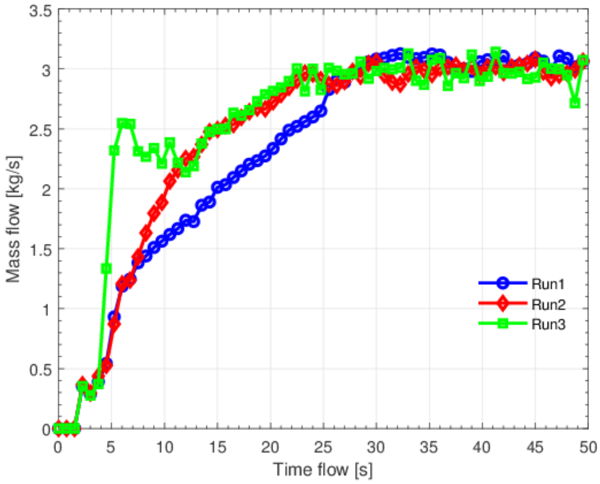

Fig. 7. Mass flow vs. time flow.

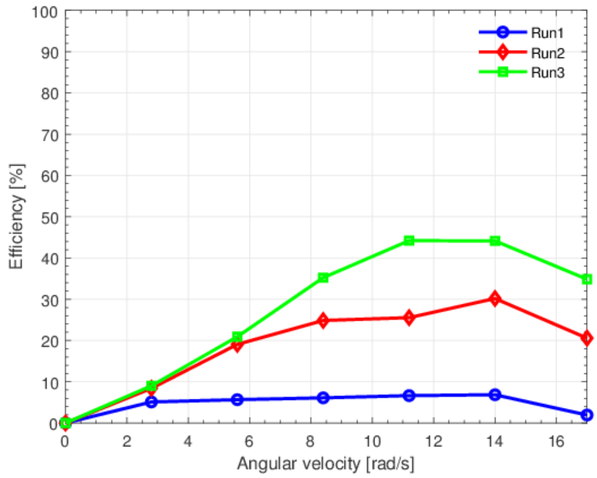

Fig. 8. Efficiency vs. angular velocity.

5. Conclusion

GWVHTs constitute a low head hydropower technology. The requirements for their implementation are lower than those ones of conventional turbines, since no major civil works are needed, the electricity produced by this method can be considered renewable and have slight negative environmental impacts associated.

According to the numerical results, the maximum efficiency (44.15%) was established when the runner was located at 60% of the basin height. An experimental verification of the optimal model will be necessary to validate the numerical results. For future works, further numerical and experimental studies should be conducted to establish the optimal runner design for GWVHT, including not only the position of the rotor in the basin but also the number of blades, the inlet, and the outlet angles, as well as the helical pitch angle and the rotor diameters and height.

Acknowledgement

We acknowledge the financial support provided by the announcement No. 890 de 2020 "Convocatoria para el fortalecimiento de CTeI en Instituciones de Educación de Educación Superior (IES) Públicas 2020" (Contract No. 2022-0453). Additionally, authors acknowledge the financial support provided by Universidad de Antioquia (Estrategia de Sostenibilidad 2020-2021. ES84190067).

References

[1] Jonsson, D. K., Gustafsson, S., Wangel, J., Höjer, M., Lundqvist, P., & Svane, Ö. (2011). Energy at your service: highlighting energy usage systems in the context of energy efficiency analysis. Energy Efficiency, 4(3), 355-369.
[2] Bakirtas, T., & Akpolat, A. G. (2018). The relationship between energy consumption, urbanization, and economic growth in new emerging-market countries. Energy, 147, 110-121.
[3] Ellabban, O., Abu-Rub, H., & Blaabjerg, F. (2014). Renewable energy resources: Current status, future prospects and their enabling technology. Renewable and Sustainable Energy Reviews, 39, 748-764.
[4] Breeze, P. (2018). Hydropower. Academic Press.
[5] Kapoor, R. (2013). Pico Power: A boon for rural electrification. International Journal of Scientific Research, 2(9), 159-161.
[6] Velásquez, L., Chica, E., & Posada, J. (2021). Jestr r. Journal of Engineering Science and Technology Review, 14(3), 1-14.
[7] Timilsina, A. B., Mulligan, S., & Bajracharya, T. R. (2018). Water vortex hydropower technology: a state-of-the-art review of developmental trends. Clean Technologies and Environmental Policy, 20(8), 1737-1760.
[8] Paish, O. (2002). Small hydro power: technology and current status. Renewable and Sustainable Energy Reviews, 6(6), 537-556.
[9] Quaranta, E. (2019). Optimal rotational speed of Kaplan and Francis turbines with focus on low-head hydropower applications and dataset collection. Journal of Hydraulic Engineering, 145(12), 04019043.
[10] Chan, C. W., Seville, J. P., Fan, X., & Baeyens, J. (2009). Particle motion in CFB cyclones as observed by positron emission particle tracking. Industrial & Engineering Chemistry Research, 48(1), 253-261.
[11] Dhakal, S., Timilsina, A. B., Dhakal, R., Fuyal, D., Bajracharya, T. R., Pandit, H. P., & Nakarmi, A. M. (2015). Comparison of cylindrical and conical basins with optimum position of runner: Gravitational water vortex power plant. Renewable and Sustainable Energy Reviews, 48, 662-669.
[12] Bajracharya, T. R., Shakya, S. R., Timilsina, A. B., Dhakal, J., Neupane, S., Gautam, A., & Sapkota, A. (2020). Effects of geometrical parameters in gravitational water vortex turbines with conical basin. Journal of Renewable Energy, 2020.
[13] Velásquez, L., Posada, A., & Chica, E. (2022). Optimization of the basin and inlet channel of a gravitational water vortex hydraulic turbine using the response surface methodology. Renewable Energy, 187, 508-521, ISSN 0960-1481, https://doi.org/10.1016/j.renene.2022.01.113.
[14] Dhakal, R., Bajracharya, T. R., Shakya, S. R., Kumal, B., Williamson, S., Khanal, K., Gautam, S., & Ghale, D. P. (2018). Computational and experimental investigation of runner for gravitational water vortex power plant. In 2017 IEEE 6th International Conference on Renewable Energy Research and Applications (ICRERA) (Vol. 373, p. 363).
[15] Zore, K., Caridi, D., & Lockley, I. (2020). Fast and accurate prediction of vehicle aerodynamics using ANSYS mosaic mesh (No. 2020-01-5011). SAE Technical Paper.
[16] Zore, K., Azab, M., Sasanapuri, B., Shah, S., & Stokes, J. (2019, August). ANSYS scale resolving simulations of launch-vehicle configuration at transonic speeds. In 21st Annual CFD Symposium (pp. 8-9).
[17] Phillips, T. S., and Roy, C. J. (2014). Richardson Extrapolation-Based Discretization Uncertainty Estimation for Computational Fluid Dynamics. Journal of Fluids Engineering, 136 (12), https://doi.org/10.1115/1.4027353
[18] Baker, N., Kelly, G., & O'Sullivan, P. D. (2020). A grid convergence index study of mesh style effect on the accuracy of the numerical results for an indoor airflow profile. International Journal of Ventilation, 19(4), 300-314.
[19] Velásquez, L., Jaramillo, L. Y., Chica, E., & Rubio-Clemente, (2020). Numerical analysis of the inlet channel and basin geometries for vortex generation in a gravitational water vortex power plant. Renewable Energy and Power Quality Journal. 18. 161-166. 10.24084/repqj18.259.
[20] Saleem, A. S., Cheema, T. A., Ullah, R., Ahmad, S. M., Chattha, J. A., Akbar, B., & Park, C. W. (2020). Parametric study of single-stage gravitational water vortex turbine with cylindrical basin. Energy, 200, 117464.
[21] Khan, N. H., Cheema, T. A., Chattha, J. A., & Park, C. W. (2018). Effective basin–blade configurations of a gravitational water vortex turbine for microhydropower generation. Journal of Energy Engineering, 144(4), 04018042.
[22] Gautam, A., Sapkota, A., Neupane, S., Dhakal, J., Timilsina, A. B., & Shakya, S. (2016, August). Study on effect of adding booster runner in conical basin: gravitational water vortex power plant: a numerical and experimental approach. In Proceedings of IOE graduate conference (pp. 107-113).
[23] Wardhana, E. M., Santoso, A., & Ramdani, A. R. (2019). Analysis of Gottingen 428 airfoil turbine Propeller Design with Computational Fluid dynamics method on gravitational water vortex power plant. International Journal of Marine Engineering Innovation and Research, 3(3).
[24] Ullah, R., Cheema, T. A., Saleem, A. S., Ahmad, S. M., Chattha, J. A., & Park, C. W. (2019). Performance analysis of multi-stage gravitational water vortex turbine. Energy Conversion and Management, 198, 111788.